(Received 12 February 2024, Accepted 19 March 2024, Scheduled 30 March 2024)

A Novel Filter with Reconfigurable Bandwidth or Transmission Zeros Based on a Multiple-Mode Stub-Loaded Resonator

Liangzu Cao* and Shouzhan Li

School of Mechanical and Electronic Engineering, Jingdezhen Ceramic University, Jingdezhen, China

ABSTRACT: This paper presents a novel bandpass filter with reconfigurable bandwidth or transmission zeros. The proposed filter is based on a multiple-mode stub-loaded resonator. Three PIN diodes are utilized as switching elements to achieve four switchable operating states. The measurement results indicate that the 3 dB fractional bandwidth (FBW) of the filter can be varied from 32.3% to 70% at the centre frequency of 2.2 GHz, and the stopband attenuation is higher than 35 dB. The filter size is only about $0.28\lambda g \times 0.19\lambda g$.

1. INTRODUCTION

In the face of increasingly scarce spectrum resources, the realization of more powerful reconfigurable filters in limited circuit spaces has always been a research focus. Reconfigurable bandwidth filters are particularly useful in the design of high-frequency multifunction receivers that simultaneously support multiple information signals with different frequency bands and power level characteristics [1, 2]. Various high-performance bandwidth reconfigurable filters have been designed by using varactor diodes [3–5] and PIN diodes [6–14] as tunable components. In [6], a bandwidth reconfigurable filter was implemented by using Semi-conductor Distributed Doped Areas (ScDDAs) as an integrated element to convert the resonator from a $\lambda/2$ open stub to a $\lambda/4$ stub. In [7], PIN diodes were used to control the connection status of the stub to achieve five switchable bandwidth states. In [8], four PIN diodes were used to achieve three bandwidth states. In [9, 10], reconfigurable bandwidth filters were designed based on a stub-loaded ring resonator. In [11], a PIN diode was used to control the connection state of two bent $\lambda/4$ resonators and one $\lambda/2$ resonator, which can be switched between wide band and narrow band. In [12], bandwidth reconfiguration was achieved by loading PIN diodes to change the length of the coupling stub. In addition, there are some studies on transmission zeros (TZs) reconfigurable filters [15, 16]. In [15], reconfigurable transmission zeros were achieved by controlling the relative positions of odd-/even-mode frequencies. In [16], transmission zero was reconfigured by changing the inter-stage coupling type using varactors.

In this article, a bandpass filter with reconfigurable bandwidth or transmission zeros is proposed. The wideband response is achieved by a multiple-mode square ring loaded resonator, and the passband bandwidth is reconfigured by switching three short-stubs loaded on the multi-mode resonator. The introduction of source-load coupling and the change of coupling type between resonators result in reconfigurable transmission zeros. A prototype is designed, fabricated, and measured to validate the approach. It will have good application prospects in the new generation of wideband and reconfigurable communication systems, such as 5G and 6G systems.

2. DESIGN PROCEDURE

Figure 1 shows the layout of the proposed reconfigurable filter. Three short-circuited stubs are connected through three PIN diodes $D1$, $D2$, and $D3$ to control the connection state and achieve the reconfigurable response states. In addition, capacitors C_b and RF-choke inductors L are used to block the DC voltage and bypass the used radio frequency (RF) signal, respectively.

$D1$, $D2$ and $D3$ are used to change the frequency response of the proposed filter. Table 1 lists the operation states.

2.1. Analysis of Multiple-Mode Resonator (Case A)

In case A, all short-circuited stubs are disconnected from the resonator, and the filter consists of a multiple-mode resonator loaded with a square ring (SRLR), which can generate multiple resonant modes required for wideband response. Fig. 2 shows the basic structure of SRLR, where the influence of bias circuits is ignored. Since the resonator is symmetrical to the central plane, the odd- and even-mode analysis method can be used. The electric wall (EW) or magnetic wall (MW) appears on the symmetry plane in Fig. 2, respectively, and we obtain the equivalent circuits for odd- and even-mode without I/O coupling, as shown in Figs. 3(a) and (b).

Based on the transmission line theory, the odd-mode input admittance Y_{inodd} and even-mode input admittance Y_{ineven} can be derived as

$$Y_{inodd} = Y_1 \frac{Y_{odd} + jY_1 \tan\theta_1}{Y_1 + jY_{odd} \tan\theta_1} \quad (1)$$

* Corresponding author: Liangzu Cao (clz4233@aliyun.com).

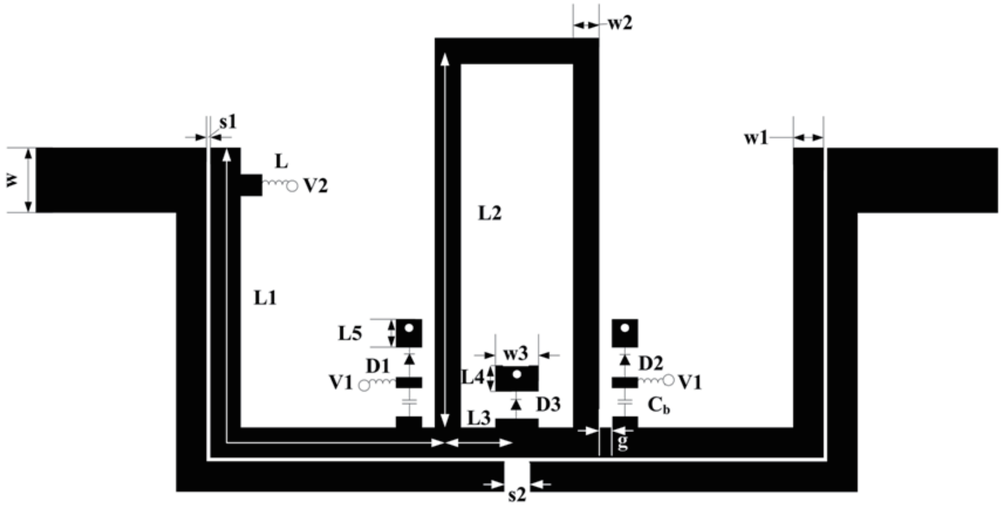

FIGURE 1. Layout of the proposed reconfigurable filter. $w = 3$, $w1 = 1.4$, $w2 = 1.2$, $w3 = 2$, $L1 = 27.2$, $L2 = 18$, $L3 = 2.6$, $L4 = 0.8$, $L5 = 0.8$, $g = 0.6$, $s1 = 0.1$, $s2 = 1$, units: mm.

TABLE 1. Operation states of the proposed filter.

	Case A	Case B	Case C	Case D
$D1$, $D2$	Off	Off	On	On
D3	Off	On	Off	On
pole	Two	Three	Two	Three
TZ	Two	One	Three	One
Location of TZ	higher stopband	lower stopband	both stopband	lower stopband
BW	Medium	Wide	Medium	Narrow

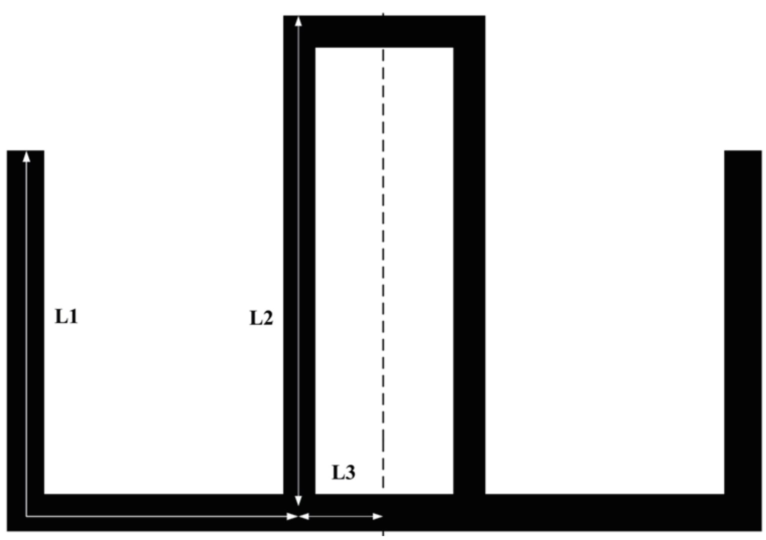

FIGURE 2. Basic structure of the SRLR.

$$Y_{ineven} = Y_1 \frac{Y_{even} + jY_1 \tan\theta_1}{Y_1 + jY_{odd} \tan\theta_1} \tag{2}$$

where

$$Y_{odd} = -jY_1 \cot\theta_3 - jY_2 \cot(\theta_2 + \theta_3) \tag{3}$$

$$Y_{even} = jY_1 \tan\theta_3 + jY_2 \tan(\theta_2 + \theta_3) \tag{4}$$

Substituting (3) into (1) and (4) into (2), we get (5) and (6),

$$Y_{inodd} = jY_1 \frac{Y_1 \tan\theta_1 - Y_1 \cot\theta_3 - Y_2 \cot(\theta_2 + \theta_3)}{Y_1 + Y_1 \tan\theta_1 \cot\theta_3 + Y_2 \tan\theta_1 \cot(\theta_2 + \theta_3)} \tag{5}$$

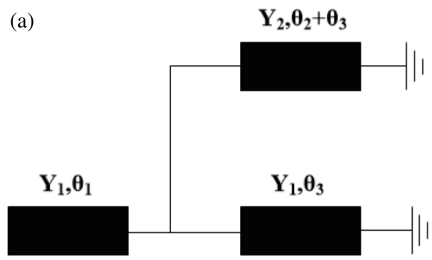

FIGURE 3. Equivalent circuits of the SRLR. (a) Odd-mode. (b) Even-mode.

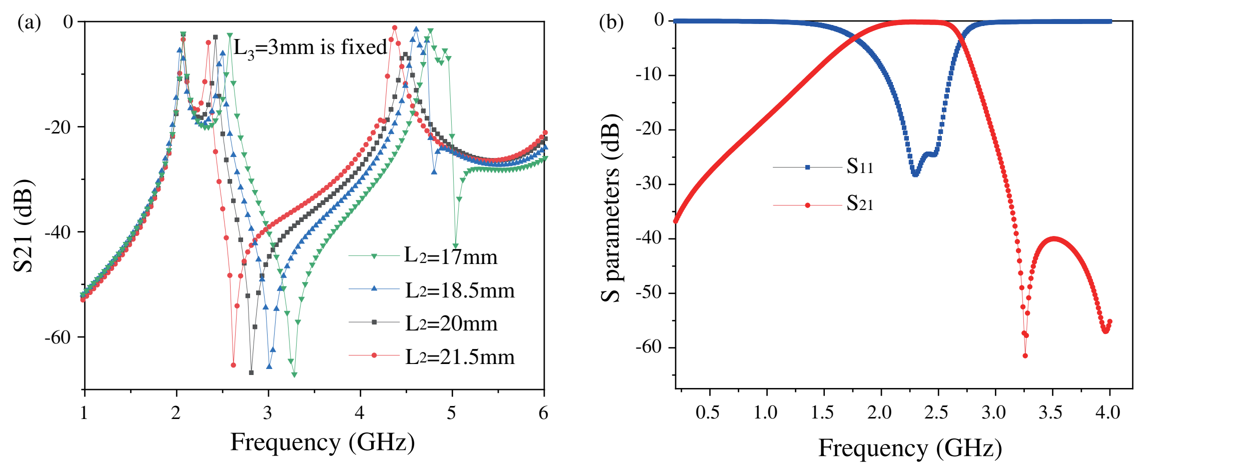

FIGURE 4. (a) Effect of L_2 on the odd-mode and even-mode resonant frequencies. (b) Simulated results of two-pole bandpass response (case A).

$$Y_{inodd} = jY_1 \frac{Y_1 \tan\theta_1 + Y_1 \tan\theta_3 + Y_2 \tan(\theta_2+\theta_3)}{Y_1 - Y_1 \tan\theta_1 \tan\theta_3 - Y_2 \tan\theta_1 \tan(\theta_2+\theta_3)} \quad (6)$$

where $\theta_1 = \beta L_1, \theta_2 = \beta L_2, \theta_3 = \beta L_3$, and β is the propagation constant; Y_1 and Y_2 denote the characteristic admittances of the corresponding transmission lines L_1, L_2 and L_3, respectively.

In order to accurately analyze the odd- and even-mode, the odd-mode resonance condition can be derived by setting $Y_{\text{inodd}} = 0$. From (5), the odd-mode frequency can be deduced as

$$Y_1 \tan\theta_1 - Y_1 \cot\theta_3 - Y_2 \cot(\theta_2+\theta_3) = 0 \quad (7)$$

Similarly, the even-mode resonance condition can be derived by setting $Y_{\text{ineven}} = 0$. From (6), the even-mode frequency can be deduced as

$$Y_1 \tan\theta_1 + Y_1 \tan\theta_3 + Y_2 \tan(\theta_2+\theta_3) = 0 \quad (8)$$

From (7), two odd-mode frequencies f_{o1} and f_{o2} can be obtained. Similarly, from (8), two even-mode frequencies f_{e1} and f_{e2} can be produced, and they are influenced by the electrical lengths θ_1, θ_2, and θ_3.

The simulated results show that $f_{\text{o2}}/f_{\text{o1}}$ and $f_{\text{e2}}/f_{\text{e1}}$ are greater than 1.5, so the proposed structure usually is designed as a dual-band bandpass filter [17], and can also be designed as a wideband filter by adjusting the electrical lengths θ_2 and θ_3 [18].

Assume that the substrate dielectric constant is 2.2, and the thickness is 1 mm. Let $w_1 = 1.2$ mm ($Z_1 = Z_2 = Z_3 = 85\,\Omega$) and $L_1 + L_3 = 25.8$ ($\theta_1 + \theta_3 = 90°$ at 2.2 GHz), and the effect of $L_2(\theta_2)$ on the odd-mode and even-mode resonant frequencies is discussed. Fig. 4(a) shows the frequency responses under a weak I/O coupling.

It is observed that when L_2 increases, the even-mode resonant frequency f_{e1} decreases while the odd-mode resonant frequency f_{o1} basically remains unchanged.

Figure 4(b) shows the simulated result of the filter with $\theta_2 = 62.8°$, $\theta_3 = 10.5°$. The 3 dB FBW is 42% (1.76–2.7 GHz), with an insertion loss of 0.2 dB and a return loss better than 24.5 dB. Two TZs appear on the right side of the passband. One TZ is produced by the multiple-mode resonator and the other produced by the load-source cross coupling.

2.2. Analysis of Case B

In case B, the diode $D3$ is turned on, and $D1$ and $D2$ are turned off. The proposed reconfigurable filter operates in wideband bandpass mode. Fig. 5(a) shows the effect of the length $L4$ of the short-circuited stub on the resonant frequencies under a weak I/O coupling.

It is observed that three resonant frequencies, including one odd-mode frequency and two even-mode frequencies appear, $f_{\text{e1}} < f_{\text{o1}} < f_{\text{e2}}$. When the length L_4 of the short-circuited

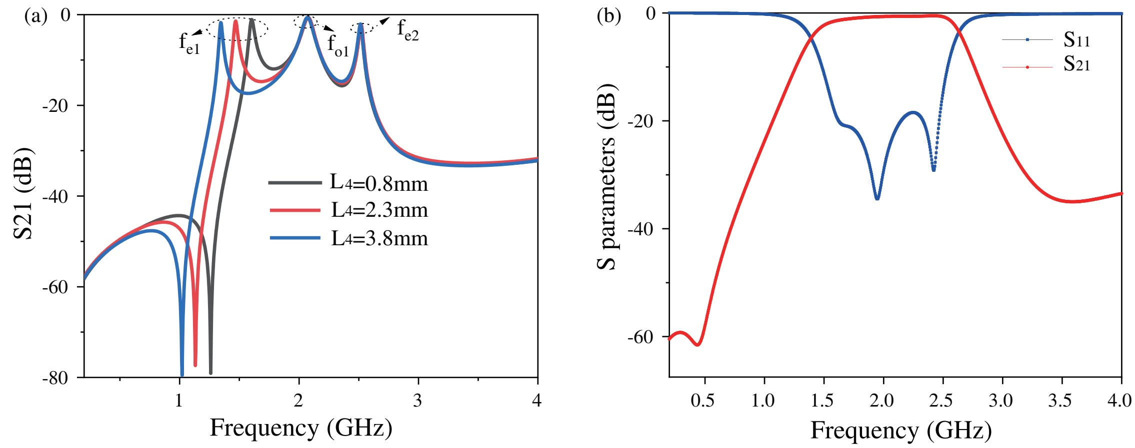

FIGURE 5. (a) Effect of different L_4 on resonant frequencies (state B). (b) Simulated results of wideband bandpass response (case B).

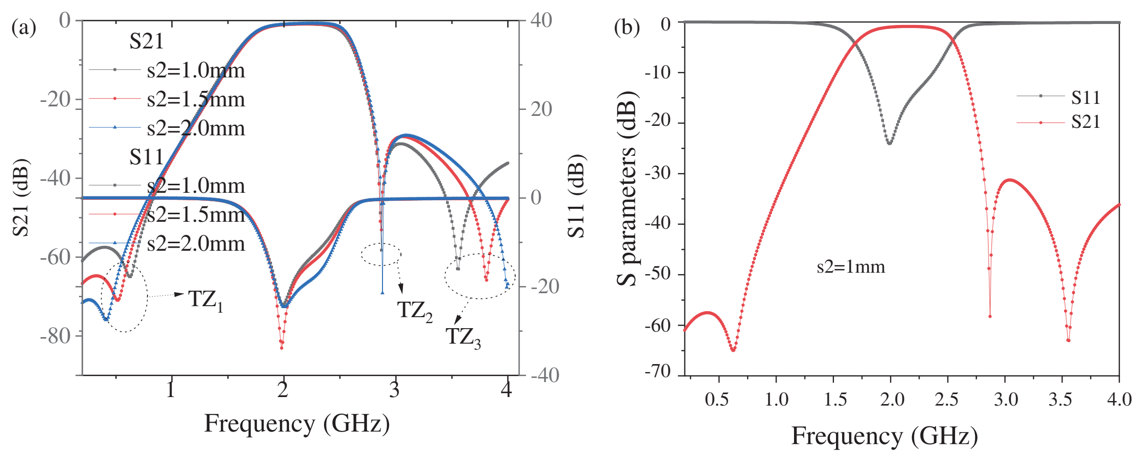

FIGURE 6. (a) Effect of different s2 on TZs. (b) Simulated results of two-pole bandpass response (case C).

stub increases, the first even-mode frequency f_{e1} shifts towards the low frequency, while the other two frequencies remain unchanged. In addition, a transmission zero (TZ) appears in the lower stopband, but the TZs in the higher stopband disappear.

Figure 5(b) shows the simulated results of the wideband bandpass response. The 3 dB FBW is 60% (1.4–2.6 GHz), while the in-band insertion loss is 0.5 dB, and the return loss within the passband is higher than 18.5 dB. The transmission zero of the lower stopband is 0.43 GHz.

2.3. Analysis of Case C

In case C, the diode $D3$ is off, and $D1$ and $D2$ are turned on. The proposed reconfigurable filter operates in medium bandwidth mode. There are three TZs on both sides of the passband, of which TZ_1 and TZ_2 are generated by the direct coupling of the multiple-mode resonator, and TZ_3 is generated by introducing a cross coupling between the source and load. Fig. 6(a) shows the relationship between TZs and the coupling gap $s2$. It is observed that TZ_3 moves towards the passband, while the positions of TZ_1 and TZ_2 remain almost unchanged when $s2$ decreases. Fig. 6(b) shows the simulated result of the filter with a 3 dB FBW of 40% (1.7–2.55 GHz), an insertion loss of 0.8 dB, and a return loss better than 24 dB. It can be observed that there are three TZs on both sides of the passband, of which TZ_1 and TZ_2 are generated by direct coupling of the multiple-mode resonator, and TZ_3 is generated by introducing a cross coupling between the source and load.

2.4. Analysis of Case D

In case D, all diodes are turned on, the proposed reconfigurable filter operates in narrowband bandpass mode.

Figure 7(a) shows the effect of the length $L5$ of the short-circuited stub on the resonant frequencies under a weak I/O coupling. When the length $L5$ decreases, the first two resonant frequencies f_{e1} and f_{o1} move towards high frequency together, while f_{e2} basically remains unchanged. Therefore, choosing appropriate the length $L5$ can achieve a narrowband bandpass response.

Figure 7(b) shows the simulated results of narrowband bandpass response. The 3 dB FBW is 8.9% (2.35–2.57 GHz), with an in-band insertion loss of 0.6 dB and a return loss greater than 20 dB. There are two TZs on both sides of the passband, which allows the filter to achieve attenuation levels above 52.5 dB and 34 dB in the lower and upper stopbands, respectively.

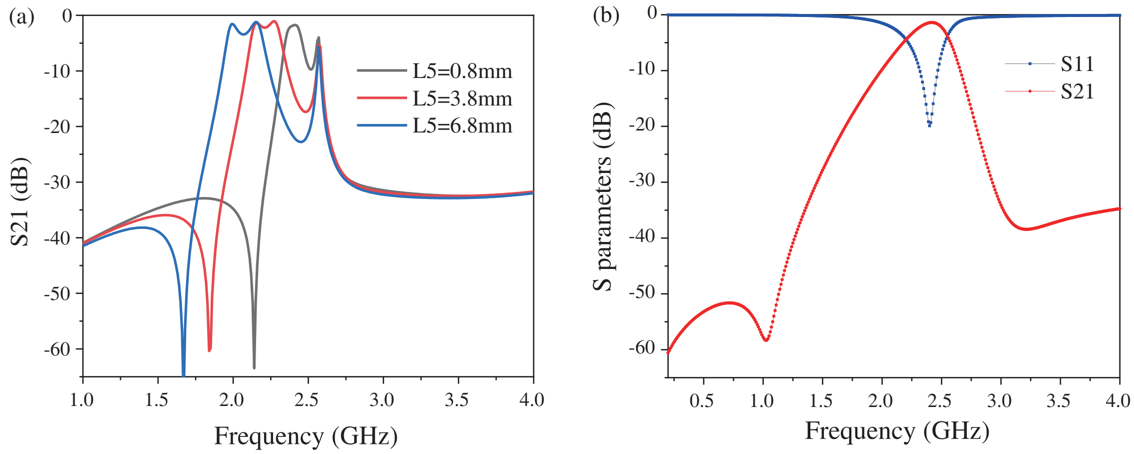

FIGURE 7. (a) Effect of different L_5 on resonant frequencies. (b) Simulated results of narrowband bandpass response (case D).

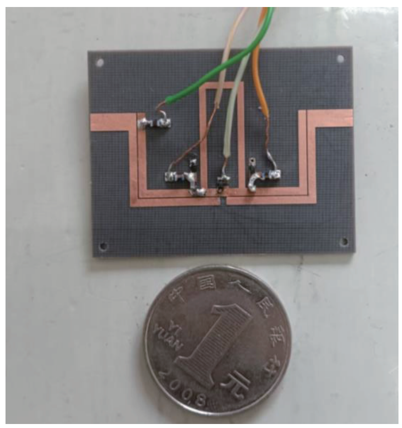

FIGURE 8. Photograph of the fabricated reconfigurable filter.

TABLE 2. Measured results of the proposed filter.

State	No. of TZ	3 dB FBW (%)	IL. (dB)	Stopband attenuation
State A	2	35.8	0.6	> 35 dB
State B	1	70	2.5	> 35 dB
State C	3	48.6	2.6	> 35 dB
State D	1	32.3	2.55	> 35 dB

TABLE 3. Comparison with references.

Ref.	states	diodes	3 dB FBW (%)	Reconfigurable TZ
[8]	3	4	34.8–56.5	No
[9]	2	4	58.5–75	No
[10]	3	6	37–92	No
[12]	2	2	1.5–4.8	No
[13]	N/A	10	N/A	Yes
[14]	N/A	6	5.2–18	No
[14]	N/A	12	N/A	Yes
This work	4	3	32.3–70	Yes

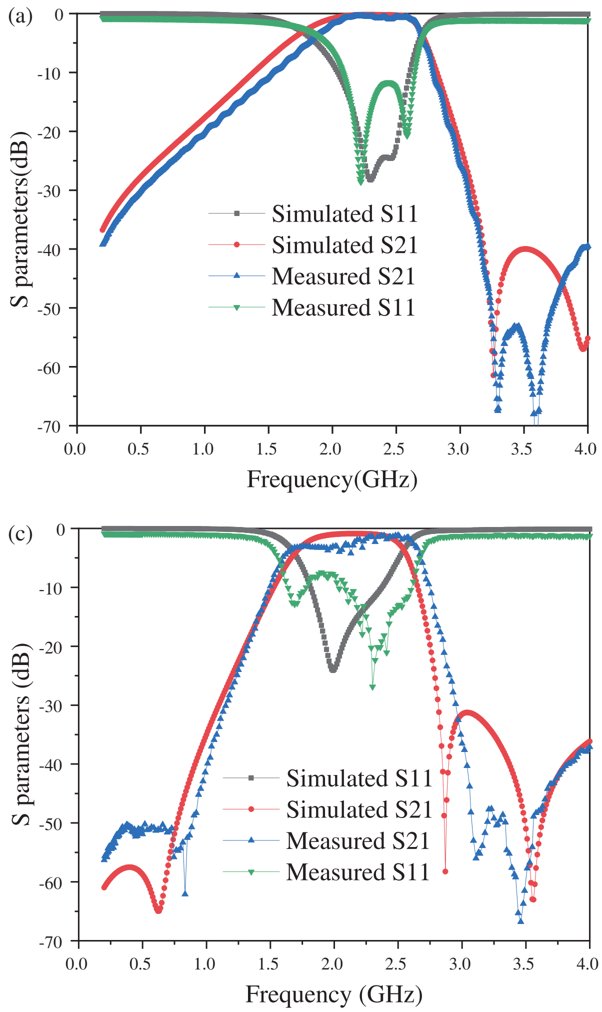

FIGURE 9. Measured results of the reconfigurable filter. (a) Case A, (b) Case B, (c) Case C, (d) Case D.

3. EXPERIMENTAL RESULTS

To verify the above design concept, a reconfigurable filter was fabricated on an F4BM substrate with a dielectric constant of 2.2 and a thickness of 1 mm.

A photograph of the fabricated reconfigurable filter is shown in Fig. 8, and the overall size of the filter is 31.4 mm × 20.9 mm ($0.28\lambda_g \times 0.19\lambda_g$) excluding the feed lines, where λ_g is the guided wavelength at the center frequency.

Three PIN diodes SMP1345-079LF ($C_T = 0.18$ pF at 5 V, $Rs = 1.5\,\Omega$ at 10 mA, $Ls = 0.7$ nH) are used as $D1$, $D2$, and $D3$ to switch filter response states. $V1$ and $V2$ are used to provide forward bias voltage for diodes $D1$, $D2$, and $D3$. 100 nH RF-choke inductors are used to connect the DC voltage. Capacitors of 47 pF are used to block the DC voltage. The filter was measured by using a vector network analyzer (Agilent E5071B). The measured results of the reconfigurable filter are shown in Fig. 9 and Table 2.

The measured transmission responses (S21) basically agree with the simulated ones. However, the measured reflection losses (S11) are worse than the simulated ones. The differences between the simulated and measured results are mainly due to the fabrication tolerances, dielectric losses, and PIN diode parasitic effects.

Compared with some other reported works, the proposed reconfigurable filter has more operating states by using fewer PIN diodes than [8–14], shown in Table 3.

It is clearly observed that the proposed filter can achieve four response states with three PIN diodes and has a wide tuning FBW range of 37.7% and the highest stopband attenuation level. In addition, the proposed filter has high selectivity performance due to reconfigurable TZs.

4. CONCLUSION

A novel filter with reconfigurable bandwidth or transmission zeros has been presented and analyzed. Four operating states are achieved by controlling the ON/OFF states of three PIN diodes. The measured and simulated results are basically consistent, which validates the design concept. This filter has the advantages of compact size, high stopband attenuations, wide tuning range for the FBW, and reconfigurable multifunction.

ACKNOWLEDGEMENT

This work was supported in part by the National Natural Science Foundation of China [grant number: 61661023]; Ph.D. research startup foundation of Jingdezhen Ceramic University of China [grant number: 2018-01].

REFERENCES

[1] Feng, W., X. Ma, Y. Shi, S. Shi, and W. Che, "High-selectivity narrow-and wide-band input-reflectionless bandpass filters with intercoupled dual-behavior resonators," *IEEE Transactions on Plasma Science*, Vol. 48, No. 2, 446–454, Feb. 2020.

[2] Feng, W., Y. Shang, W. Che, R. Gómez-García, and Q. Xue, "Multifunctional reconfigurable filter using transversal signal-interaction concepts," *IEEE Microwave and Wireless Components Letters*, Vol. 27, No. 11, 980–982, Nov. 2017.

[3] Zhu, H. and A. Abbosh, "Tunable band-pass filter with wide stopband and high selectivity using centre-loaded coupled structure," *IET Microwaves, Antennas & Propagation*, Vol. 9, No. 13, 1371–1375, 2015.

[4] Guo, H., J. Ni, and J. Hong, "Varactor-tuned dual-mode bandpass filter with nonuniform Q distribution," *IEEE Microwave and Wireless Components Letters*, Vol. 28, No. 11, 1002–1004, 2018.

[5] Lan, B., Y. Qu, C. Guo, and J. Ding, "A fully reconfigurable bandpass-to-notch filter with wide bandwidth tuning range based on external quality factor tuning and multiple-mode resonator," *Microwave and Optical Technology Letters*, Vol. 61, No. 5, 1253–1258, 2019.

[6] Allanic, R., D. L. Berre, Y. Quere, C. Quendo, D. Chouteau, V. Grimal, D. Valente, and J. Billoue, "A novel synthesis for bandwidth switchable bandpass filters using semi-conductor distributed doped areas," *IEEE Access*, Vol. 8, 122 599–122 609, 2020.

[7] Sánchez-Soriano, M. A., R. Gómez-García, G. Torregrosa-Penalva, and E. Bronchalo, "Reconfigurable-bandwidth bandpass filter within 10-50%," *IET Microwaves, Antennas & Propagation*, Vol. 7, No. 7, 502–509, 2013.

[8] Cheng, T. and K.-W. Tam, "A wideband bandpass filter with reconfigurable bandwidth based on cross-shaped resonator," *IEEE Microwave and Wireless Components Letters*, Vol. 27, No. 10, 909–911, 2017.

[9] Arain, S., P. Vryonides, M. A. B. Abbasi, A. Quddious, M. A. Antoniades, and S. Nikolaou, "Reconfigurable bandwidth bandpass filter with enhanced out-of-band rejection using π-section-loaded ring resonator," *IEEE Microwave and Wireless Components Letters*, Vol. 28, No. 1, 28–30, 2018.

[10] Arain, S., P. Vryonides, A. Quddious, and S. Nikolaou, "Reconfigurable BPF with constant center frequency and wide tuning range of bandwidth," *IEEE Transactions on Circuits and Systems II: Express Briefs*, Vol. 67, No. 8, 1374–1378, 2020.

[11] Karim, M. F. and M. Y. Siyal, "A compact switchable and tunable bandpass filter," *Progress in Electromagnetics Research M*, Vol. 85, 71–81, 2019.

[12] Vryonides, P., S. Nikolaou, S. Kim, and M. M. Tentzeris, "Reconfigurable dual-mode bandpass filter within 10-50%," *International Journal of Microwave and Wireless Technologies*, Vol. 7, No. 6, 655–660, 2015.

[13] Tsai, H.-J., B.-C. Huang, N.-W. Chen, and S.-K. Jeng, "A reconfigurable bandpass filter based on a varactor-perturbed, T-shaped dual-mode resonator," *IEEE Microwave and Wireless Components Letters*, Vol. 24, No. 5, 297–299, 2014.

[14] Fu, M., Q. Feng, Q. Xiang, and N. Jiang, "Fully tunable filter with cross coupling and reconfigurable transmission zero," *International Journal of RF and Microwave Computer-Aided Engineering*, Vol. 30, No. 12, e22407, 2020.

[15] Ramkumar, S. and R. B. Rani, "Compact reconfigurable bandpass filter using quarter wavelength stubs for ultra-wideband applications," *AEU — International Journal of Electronics and Communications*, Vol. 151, 154219, 2022.

[16] Qin, P.-Y., F. Wei, and Y. J. Guo, "A wideband-to-narrowband tunable antenna using a reconfigurable filter," *IEEE Transactions on Antennas and Propagation*, Vol. 63, No. 5, 2282–2285, May 2015.

[17] Liu, H., B. Ren, X. Guan, J. Lei, and S. Li, "Compact dual-band bandpass filter using quadruple-mode square ring loaded resonator (SRLR)," *IEEE Microwave and Wireless Components Letters*, Vol. 23, No. 4, 181–183, Apr. 2013.

[18] Zhang, P., L. Liu, D. Chen, M.-H. Weng, and R.-Y. Yang, "Application of a stub-loaded square ring resonator for wideband bandpass filter design," *Electronics*, Vol. 9, No. 1, 176, 2020.